Supporting Information

Ultrahigh Responsivity UV Photodetector Enabled by Spatially Confined 2D β-Ga_2O_3/$PdSe_2$ van der Waals Heterojunction

Ruan Zhang,[a] Xianyu Hu,[b] Yunlei Zhong,[b] Xianming Li,[c] Yong Zhang,[b] Youchao Kong [d,*] Xiyuan Feng [c,*]

[a]School of Electronic and Information Engineering, Suzhou Polytechnic University, Suzhou 215104, China
[b]Advanced Materials Division, Suzhou Institute of Nano-Tech and Nano-Bionics, Chinese Academy of Sciences, Suzhou 215123, China
[c]School of Integrated Circuits (School of Microelectronics), Northwestern Polytechnical University, No. 1 Dongxiang Road, Chang' an District, Xi' an 710129, P. R. China
[d]Department of Physics and Electronic Engineering, Yancheng Teachers University, Yancheng, P.R. China
[*]Authors to whom correspondence should be addressed: fengxy@nwpu.edu.cn
kongyc@yctu.edu.cn

S1: Raman spectra of pure β-Ga_2O_3, pure $PdSe_2$ and the heterojunction.

As illustrated in Fig.S1, the Raman spectrum of the β-Ga_2O_3/$PdSe_2$ heterojunction overlapping region is essentially consistent with that of the pure $PdSe_2$. Specifically, the characteristic A_{1g} (176 cm^{-1}), B_{1g} (210 cm^{-1}), and A_{2g} (303 cm^{-1}) vibrational modes of $PdSe_2$ remain well-resolved, showing no obvious peak shift or broadening compared to the pure component. In contrast, the characteristic Raman peaks of β-Ga_2O_3 in the heterojunction region are almost undetectable. This phenomenon likely originates from two core factors and reveals critical interfacial properties of the β-Ga_2O_3/$PdSe_2$ van der Waals heterojunction:

(1) Weak interfacial interaction without chemical bonding: The negligible variation in $PdSe_2$'s Raman peaks indicates that the formation of the heterojunction does not induce obvious lattice distortion or strong chemical bonding at the interface. The intrinsic crystal structure of $PdSe_2$ is well preserved—a hallmark of high-quality van der Waals heterojunctions dominated by weak van der Waals forces. This avoids the generation of interfacial defect states caused by chemical bonding or lattice mismatch, laying a solid foundation for efficient carrier transport;

(2) Optical absorption dominance of $PdSe_2$: The undetectable Raman peaks of β-Ga_2O_3 in the heterojunction region are mainly attributed to the higher optical absorption coefficient of $PdSe_2$ at the 532 nm excitation wavelength (used for Raman testing) compared to β-Ga_2O_3. The incident laser is predominantly absorbed by the $PdSe_2$ layer, leading to the suppression of β-Ga_2O_3's Raman signal. This is a common optical phenomenon in van der Waals heterostructures with asymmetric optical absorption, rather than a reflection of the interfacial coupling strength[1].

Notably, the weak van der Waals interfacial interaction observed in Raman characterization is fully consistent with the atomically sharp, defect-free interface revealed by cross-sectional STEM

imaging (Fig. 2a). This clean interface minimizes trap-assisted recombination and provides a smooth channel for carrier transfer, which is directly verified by the device's ultralow dark current and high photo-to-dark current ratio.

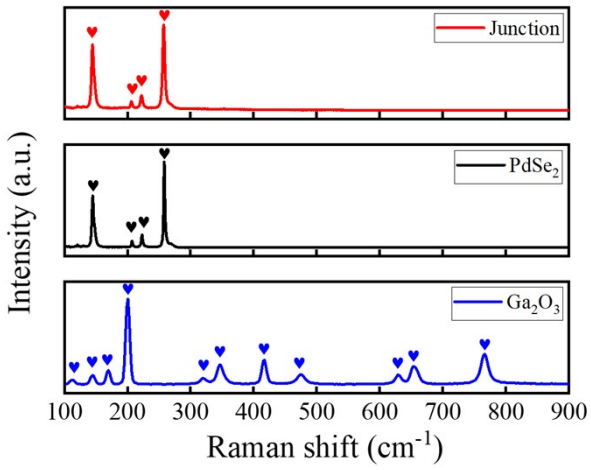

Fig. S1 Raman spectra of β-Ga_2O_3, $PdSe_2$ and the junction.

S2: Performance comparison of representative β-Ga_2O_3-based photodetectors operating in photoconductive mode.

Table S1 Performance comparison of representative β-Ga_2O_3-based photodetectors operating in photoconductive mode.

Device	Bias (V)	Responsivity (A/W)	Photo-to dark current ratio	Reference
MSM β-Ga_2O_3 micro-flake	30	1.68	1.37×10^3	[2]
MSM β-Ga_2O_3 films	5	14.09	4.9×10^4	[3]
β-Ga_2O_3/Nb_2C	5	28	213	[4]
β-Ga_2O_3/NSTO	-10	43.31	20	[5]
β-Ga_2O_3/MoS_2	-10	0.00721	10^3	[6]
β-Ga_2O_3/$CsCu_2I_3$	-1	178.9	5.4×10^4	[7]
β-Ga_2O_3/Graphene	-10	14.5	3.3×10^3	[8]
β-Ga_2O_3/ $PdSe_2$	5	6.17×10^4	2.5×10^6	Our work

References:

1 Y.T. Chu, P.L. Chen, S.H. Huang, S.N.S. Yadav, W.R. Syong, C.H. Mao, Y.J. Lu, C.H. Liu, P.C. Wu, T.J. Yen, *ACS Nano*, 2025, **19**, 18545-18555.

2 S. Oh, M.A. Mastro, M.J. Tadjer, J. Kim, *ECS J. Solid State Sci. Technol.*, 2017, **6**, Q79-Q83.

3 D.-Y. Lin, D.N. Feria, S.-X. Lin, H.-C. Hsu, X.-B. Yang, T.-Y. Lin, *Mater. Today Commun.*, 2025, **45**, 112114.

4 Y. Zhang, S. Liu, R. Xu, S. Ruan, C. Liu, Y. Ma, X. Li, Y. Chen, J. Zhou, *Nanotechnology*, 2024, **35**, 165502.

5 D. Guo, H. Liu, P. Li, Z. Wu, S. Wang, C. Cui, C. Li, W. Tang, *ACS Appl. Mater. Interfaces*, 2017, **9**, 1619-1628.

6 M. Sharma, A. Singh, A. Kapoor, A. Singh, B.R. Tak, S. Kaushik, S. Bhattacharya, R. Singh, *ACS Appl. Electron. Mater.*, 2023, **5**, 2296-2308.

7 Y. Chen, Y. Li, Y. Yang, X. Yang, C. Shan, G. Shen, *Nano Energ.*, 2025, **138**, 110833.
8 M. Labed, B.I. Park, J. Kim, J.H. Park, J.Y. Min, H.J. Hwang, J. Kim, Y.S. Rim, *ACS Nano*, 2024, **18**, 6558-6569.